DOI: 10.26599/FSHW.2026.9251293

Contents lists available at SciOpen

Food Science and Human Wellness

journal homepage: https://www.sciopen.com/journal/2097-0765

China Food Publishing Co.

Exploration of the mechanism by which quorum sensing signals AI-2 and AIP enhance ethanol tolerance of *Lacticaseibacillus paracasei* 5

Mengchen Li [a], Yunhao Zhang [a], Xin Liu [a], Zhiyong Niu [a], Lin Zhang [a], Yang Mu [a], Yang Chen [a *], Junjun Gao [a], Mingye Peng [a], Mengzhou Zhou [a *]

[a] *Hubei Key Laboratory of Industrial Microbiology, Cooperative Innovation Center of Industrial Fermentation (Ministry of Education & Hubei Province), Key Laboratory of Fermentation Engineering (Ministry of Education), National "111" Center for Cellular Regulation and Molecular Pharmaceutics, Hubei University of Technology, Wuhan, Hubei, 430068, China*

ABSTRACT: *Lacticaseibacillus paracasei* (*L. paracasei*) plays an indispensable role in food fermentation and probiotic formulations. Nonetheless, its industrial utilization is frequently limited by its low tolerance to ethanol. Given that biofilm formation constitutes a critical survival mechanism for bacteria under stress conditions, this study sought to examine the impact of exogenous autoinducer-2 (AI-2) and autoinducing peptides (AIP) on the biofilm formation of *L. paracasei* in the presence of ethanol stress. The findings revealed that both AI-2 and AIP substantially enhanced biofilm formation, increased membrane fluidity, and augmented exopolysaccharide (EPS) production under ethanol stress conditions. Transcriptomic analysis further revealed distinct regulatory mechanisms: AI-2 primarily upregulated genes encoding ABC transporters (e.g., *potABCD*, *phnCDE*, *oppABCDF*), which support ATP-driven uptake of compounds essential for cellular homeostasis under ethanol stress. In contrast, AIP mainly activated genes involved in the phosphotransferase system (PTS) (e.g., *BglF*, *MtlA*, *CelB*, *CelC*), facilitating carbohydrate uptake and central carbon metabolism to meet the biosynthetic demands of EPS and biofilm matrix assembly. This work would provide important insights into the stress adaptation mechanisms mediated by quorum sensing (QS) in *L. paracasei* 5.

Keywords: *Lacticaseibacillus paracasei*; Quorum sensing; Ethanol tolerance; Biofilm; Transcriptome

1. Introduction

Lacticaseibacillus paracasei (*L. paracasei*) is recognized for its beneficial effects on gut microbiota, immune function, and protection against various health issues[1, 2]. However, its industrial use is limited by its sensitivity to environmental stresses like low pH, bile salts, oxidative stress, and ethanol[3, 4]. Ethanol stress, common in processes like wine or sake fermentation, can damage *L. paracasei* by affecting membrane integrity, protein structure, metabolism, and cell viability, leading to fermentation issues[5]. For instance, during wine or sake fermentation, lactic acid bacteria (LAB) are subjected to increasing ethanol concentrations during the essential malolactic fermentation stage. This ethanol stress can severely compromise cellular viability, causing premature fermentation arrest[6]. Therefore, its ability to withstand ethanol stress is crucial for its industrial application.

***Corresponding author**
20231134@hbut.edu.cn(Y. Chen).
zmzkelvin@hbut.edu.cn(M.Z. Zhou)

Received 13 February 2026
Received in revised from 30 March 2026
Accepted 11 May 2026

Faced with such stressors, bacteria have evolved sophisticated adaptive strategies, among which biofilm formation represents a highly effective communal survival mechanism. Biofilms are structured microbial communities embedded within a self-produced extracellular polymeric matrix (composed of EPS, proteins, and extracellular DNA), which confers enhanced resistance to environmental stresses[7]. Notably, biofilm-forming bacteria have been shown to exhibit greater ethanol tolerance compared to their planktonic counterparts, as the biofilm matrix can reduce ethanol diffusion and enhance cellular membrane stability[8]. Biofilm formation is not merely a passive physicochemical adhesion process but a developmentally regulated behavior under precise genetic control. In this process, the quorum sensing (QS) system plays a critical regulatory role in activating biofilm-associated protective pathways. QS serves as a central regulator in the process of transitioning from planktonic existence to a communal biofilm lifestyle, facilitating collective action across the bacterial population[9]. In Gram-positive bacteria such as *L. paracasei*, QS is mainly mediated by AIP and AI-2, where AIP facilitates intraspecific communication, while AI-2 serves as a universal signal for interspecific dialogue[10-16]. When the concentration of these signaling molecules reaches a threshold corresponding to a critical cell density, they trigger transcriptomic reprogramming, including the expression of biofilm-related genes[17]. This regulates the transition from a free-living state to surface attachment and ultimately to mature biofilm development. Recent studies have further revealed that exogenous supplementation of QS signaling molecules can directly influence biofilm biomass and structural stability, thereby enhancing stress resistance[18]. Nevertheless, in *L. paracasei*, it remains unclear whether and how ethanol stress affects specific QS pathways to regulate biofilm formation and ultimately determine ethanol tolerance phenotypes. This limitation restricts the application of *L. paracasei* in high-ethanol fermentation environments.

This study investigated the effects of exogenous AI-2 and AIP on biofilm formation and ethanol tolerance in *L. paracasei* 5. Transcriptomic analysis revealed the underlying mechanisms by which AI-2 and AIP regulate biofilm assembly. These findings provide novel insights into the interplay between bacterial stress responses and social behavior, while establishing a foundation for novel strategies to enhance industrial strain robustness through QS modulation.

2. Materials and Methods

2.1 Materials and reagents

L. paracasei 5 was provided by the Research Center of Food Fermentation Engineering and Technology (Hubei, China). *L. paracasei* 5 was grown in de Man, Rogosa, and Sharpe (MRS) broth at 37 ℃ for 24 h. *Vibrio harveyi* BB170 (BNCC 337376) was purchased from Chuanglian Biotechnology Co., Ltd. (Beijing, China). The *Escherichia coli* strains DH5*α* and Transetta (DE3) were cultured in Luria-Bertani (LB) broth at 37 ℃ with aeration and were used for recombinant gene cloning and protein expression, respectively. The pET28a plasmid was acquired from Genewiz Biotechnology Co., Ltd. (Shandong, China). Isopropyl *β*-D-1-thiogalactopyranoside (IPTG) and D-galactose (Catalog No. D609860; ≥98% purity) were supplied by Shanghai Macklin Biochemical Co., Ltd. (Shanghai, China). AIP was synthesized by Wuhan Sanyangkaitai

Biotechnology Co., Ltd. (Wuhan, China) based on the amino acid sequence MKEKMYKVLSHLFQYVGTKQLVMCCHGILFETKIPDELKSKD. The purity of the synthetic peptides was determined by HPLC to be 96.34% (as shown in Figure S1). Ellman's reagent (Catalog No. D218200) and the TRIzol reagent kit (Catalog No. A33251) were obtained from Sigma-Aldrich (Carlsbad, USA) and Invitrogen (Carlsbad, USA), respectively. All other chemicals of analytical grade were sourced from Sinopharm Chemical Reagent Co., Ltd. (Shanghai, China).

2.2 Synthesis and determination of AI-2

The in vitro synthesis of AI-2 was performed according to established methods[19, 20]. Expression vectors for the *LuxS* and *Pfs* genes were constructed by cloning the respective *E. coli* genes into a prokaryotic protein expression vector. Recombinant *LuxS* and *Pfs* proteins were produced by growing the host cells at 37 ℃ with aeration and inducing with 0.1 mM IPTG. The proteins were subsequently isolated and purified using a His-tag protein purification kit (Shanghai, China). For AI-2 synthesis, the purified recombinant *LuxS* and *Pfs* proteins (1 mg/mL) were combined with 1 mM S-adenosylhomocysteine (SAH) in 10 mM sodium phosphate buffer (pH 8.0) and incubated at 37 ℃ for 1 h. The AI-2 concentration was determined by measuring the homocysteine concentration via Ellman's method, with the absorbance monitored at 412 nm. Notably, the enzymatic conversion of SAH by *Pfs* and *LuxS* yields AI-2 and homocysteine in a 1:1 molar ratio. Consequently, the concentration of homocysteine serves as a direct indicator of the amount of AI-2 produced. The AI-2 activity was ultimately confirmed using the *Vibrio harveyi* BB170 bioassay.

2.3 Effects of exogenous signal molecules on the growth and biofilm of L. paracasei 5 under different ethanol concentrations

L. paracasei 5 was inoculated at 2% (v/v) into MRS broth containing various ethanol concentrations (0%, 4%, 6%, 8%, 10%, 12%) and incubated at 37 ℃. The cultures were supplemented with either *in vitro*-synthesized AI-2 (50 μmol/L) or AIP (1 μg/mL). At 24, 48, and 72 h, the growth of *L. paracasei* 5 was assessed by measuring the optical density at 600 nm using a UV–visible spectrophotometer (UV-1800, Shimadzu, Japan). Biofilm formation was assessed by crystal violet staining as described [20]. Briefly, *L. paracasei* 5 was added to a 96-well plate and incubated at 37 ℃ for 24 h. After washing with PBS, the wells were sequentially stained with 0.1% crystal violet and destained with an ethanol-acetone (4:1) solution. The biofilm biomass was quantified by measuring the absorbance of the destaining solution at 590 nm. We employed OD_{600} measurements to evaluate the dynamics of population growth, recognizing that this approach indicates alterations in total biomass without differentiating between various physiological states.

2.4 Observation of biofilm morphology

The sample preparation for scanning electron microscopy (SEM) was performed according to the method of Chabela et al. with modifications[21]. Briefly, glass coverslips were placed in a 6-well plate and inoculated with 1 mL of a bacterial suspension (1:100 in MRS) per well. After a 72 h incubation with the bacterial solution and signaling molecules, the coverslips were fixed with 2.5% glutaraldehyde for 4 h at 4 ℃. The fixed

samples were then dehydrated through a graded ethanol series (50%, 60%, 70%, 80%, 90%, 95%, and 100%), remaining in each concentration for 15 min. Finally, the samples were dried, sputter-coated with gold layer, and examined by SEM.

2.5 The influence of exogenous signaling molecules on the cell membrane fluidity of L. paracasei 5

Membrane fluidity was assessed using the small molecular probe 1,6-diphenyl-1,3,5-hexatriene (DPH)[22]. *L. paracasei* 5 were harvested by centrifugation at 5000 g for 5 min and resuspended with PBS. The suspension was then incubated with 2 μmol/L DPH at 30 ℃ for 1.5 h. Fluorescence measurements were performed on a spectrofluorometer with an excitation wavelength of 358 nm and an emission wavelength of 429 nm. Background correction was applied using a cell suspension without DPH. Fluorescence anisotropy was calculated from the differences in fluorescence intensities detected by vertically and horizontally oriented polarizers, as described previously[23].

2.6 The influence of exogenous signal molecules on the extracellular polysaccharide yield of L. paracasei 5

The EPS from *L. paracasei* 5 was isolated and quantified as follows[24]. The cell-free supernatant, prepared by centrifugation, was subjected to protein removal using trichloroacetic acid (40 mg/mL final concentration) at 4 ℃ for 24 h. Following protein precipitation and centrifugation, EPS in the supernatant was precipitated with three volumes of ethanol at 4 ℃ for 24 h The crude EPS pellet was collected, dialyzed using a 14 kDa cutoff membrane, and then quantified by the phenol-sulfuric acid method. Absorbance at 490 nm was recorded after reacting samples with phenol and sulfuric acid. All measurements were taken in triplicate using a UV–visible spectrophotometer.

2.7 Effect of exogenous signaling molecules on organic acid products of L. paracasei 5

Organic acid profiles (succinic, formic, citric, malic, lactic, and acetic acids) in the supernatant of *L. paracasei* 5 cultures with exogenous signaling molecules were analyzed by HPLC. The samples were analyzed using YMC-Pack ODS-AM C18 column (250 mm× 4.6 mm, 5 μm) maintained at 25 ℃. The mobile phase flowed at 1.0 mL/min, with detection at 210 nm and a 20 μL injection volume.

2.8 Transcriptome analysis

L. paracasei 5 was inoculated into MRS medium containing 8% ethanol and the specified signaling molecules. After 24 h of anaerobic incubation at 37 ℃, bacterial cells were harvested by centrifugation at 4000 g for 10 min at 4 ℃. The cell pellets were immediately flash-frozen in liquid nitrogen and transported on dry ice to Majorbio Biopharmaceutical Co., Ltd. (Shanghai, China). To enhance the reliability and reproducibility of the transcriptomic data, all experiments were conducted in triplicate.

Following library preparation with the TruSeq^{TM} Stranded Total RNA Kit according to the Illumina protocol, cDNA fragments of 200-300 bp were size-selected via gel electrophoresis for paired-end sequencing (150 bp × 2) on an Illumina NovaSeq 3000. All downstream analyses were conducted on the Majorbio Cloud Platform. Differential expression analysis was performed using DESeq2, defining differentially expressed

genes (DEGs) as genes with a p-value < 0.05 and |log2FC| > 2. These DEGs were then functionally annotated and analyzed for enrichment in KEGG pathways.

2.9. Statistical analysis

All statistical analyses were performed using IBM SPSS Statistics (version 26.0). One-way ANOVA was used to compare more than two groups based on a single factor, while two-way ANOVA was applied to assess the effects of two independent factors across multiple groups. A p-value < 0.05 was considered statistically significant. All experiments included at least three biological replicates per strain or condition, and quantitative data are expressed as mean ± standard deviation (SD). Consistent significance annotation symbols were used across all figures: *P < 0.05, **P < 0.01, ***P < 0.001, ****P < 0.0001.

3. Results and discussion

3.1. Determination of the signaling molecule AI-2 in L. paracasei 5

The activity of the signaling molecule AI-2 was monitored using the *V. harveyi* BB170 bioluminescence reporter system. As depicted in Figure S2A, the bioluminescence intensity showed a biphasic trend, initially decreasing before rising markedly over time. At early cultivation stages, low cell density led to sub-threshold AI-2 levels, which were insufficient to activate QS, resulting in low luminescence. As the culture progressed, continuous growth and proliferation of *V. harveyi* BB170 promoted the *LuxS*-mediated synthesis and accumulation of extracellular AI-2. Once a critical threshold of AI-2 concentration was reached, QS was induced, triggering robust expression of the luciferase operon. This led to abundant production of luciferase and its substrates, ultimately accounting for the sharp increase in bioluminescence[25, 26]. Notably, the AI-2-induced bioluminescence was significantly higher in the presence of low ethanol concentrations compared to high ethanol levels. This phenomenon can be attributed to a dual mechanism. First, elevated ethanol concentrations inhibited bacterial growth, thereby reducing the population of viable cells available for both producing and responding to AI-2 signals[27]. Furthermore, ethanol acts as a membrane disruptor, it compromises the integrity of the lipid bilayer, leading to a loss of essential membrane function[28]. Together, these results indicate that the limited ethanol tolerance of *L. paracasei* 5 may be associated with the functional vulnerability of its QS system under ethanol stress. Furthermore, the AI-2 concentration measured under standard conditions (0.869 mmol/L) provides a critical reference point for subsequent interventional studies (Figure S2B).

3.2. Effect of exogenous signaling molecules on ethanol tolerance in L. paracasei 5

LAB play an indispensable role in food fermentation and probiotic formulations. However, they are inevitably exposed to various environmental stresses during natural fermentation. Ethanol stress is particularly prominent, as it not only inhibits bacterial growth and reduces viability but also disrupts biofilm formation, thereby directly compromising their application efficacy[29]. As illustrated in Figures 1A-F, the observed decline in OD_{600} with increasing ethanol concentrations unequivocally confirms the growth-inhibitory effect of ethanol on *L. paracasei* 5. However, the significant restoration of both growth and biofilm formation upon

AI-2 supplementation reveals a crucial role of this signaling molecule in stress management. This response is characterized by the collective upregulation of biosynthetic pathways for EPS, leading to enhanced biofilm assembly. This architecture serves to mitigate intracellular damage and maintain physiological homeostasis, thereby promoting survival under adverse conditions[30, 31]. In contrast, supplementation with synthetic an AIP failed to alleviate the ethanol-induced growth inhibition, as indicated by the OD_{600} across concentrations (Figures 1G-I). This marked functional divergence underscores the signal-specific nature of QS responses. Although AIP supplementation showed no significant effect on the growth yield of *L. paracasei* 5, it consistently enhanced biofilm formation across different ethanol concentrations (Figures 1J-L). These results suggest that AIP may enhance structural resistance to ethanol stress by activating biofilm-specific gene expression pathways rather than by promoting growth. It is important to acknowledge that, although crystal violet staining is a robust and standardized technique for quantifying total biofilm biomass, it does not differentiate between viable cells, dead cells, and EPS. Nonetheless, given that all experimental and control groups were subjected to identical crystal violet staining protocols, the significant differences observed in absorbance values accurately represent relative alterations in the overall biofilm architecture resulting from the various treatments. Consequently, the reported enhancement in biofilm formation under ethanol stress reflects an increase in total biofilm structural integrity rather than solely an increase in viable cell mass.

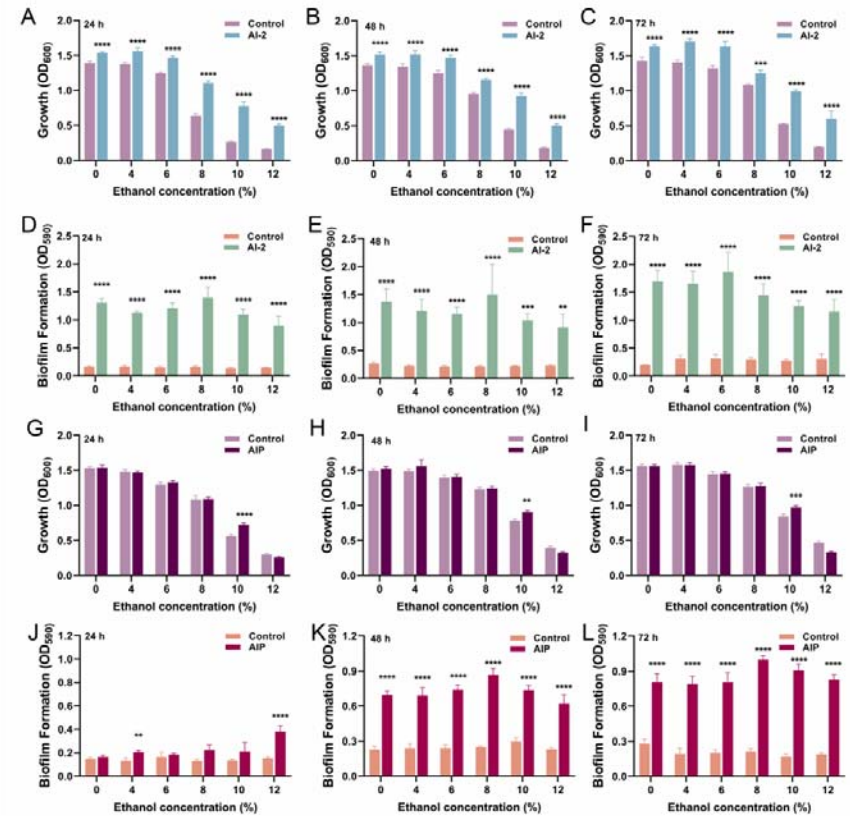
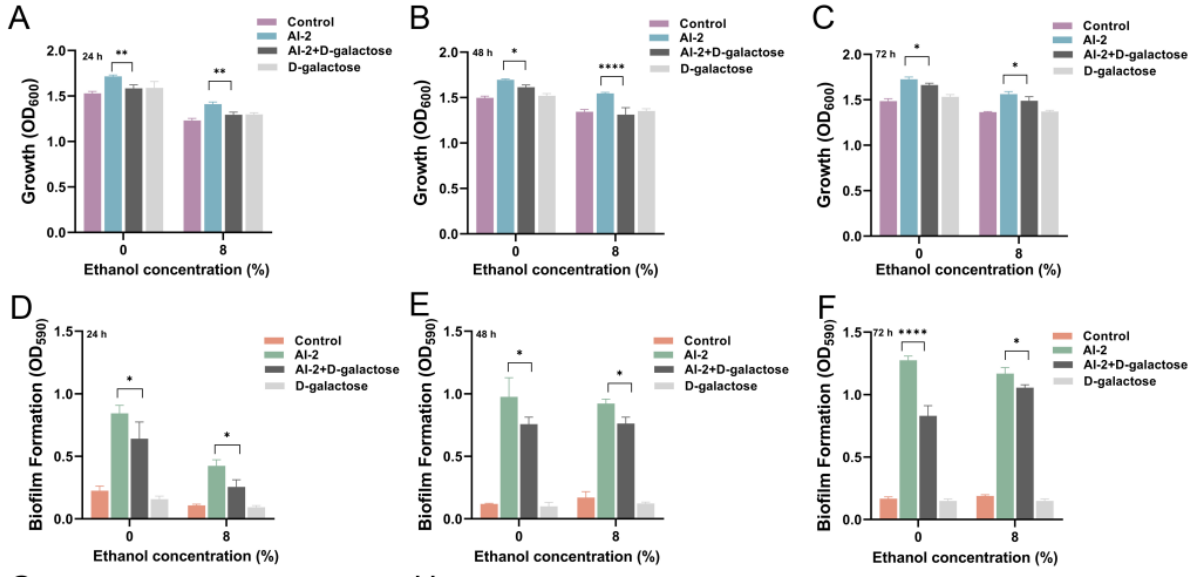


Figure 1. Effects of AI-2 and AIP on the growth and biofilm formation of *L. paracasei* 5 under ethanol stress.(A-C) Growth curves of the control and AI-2-treated groups under ethanol concentrations of 0%,4%, 6%, 8%, 10%, and 12% (v/v) at 24, 48, and 72 h, respectively. (D-F) Biofilm formation of the control and AI-2-treated groups under the same conditions. (G-I) Growth curves of the control and AIP-treated groups under ethanol concentrations of 0%, 4%, 6%, 8%, 10%, and 12% (v/v) at 24, 48, and 72 h, respectively. (J-L) Biofilm formation of the control and AIP-treated groups under the same conditions. Data were presented as mean ± SD (n = 3). Significant differences were determined by two-way ANOVA. *: $P < 0.05$, **: $P < 0.01$, ***: $P < 0.001$, ****: $P < 0.0001$.

When the extracellular AIP concentration reaches a threshold, AIP binds to the membrane-associated receptor kinase *AgrC,* resulting in phosphorylation of the response regulator *AgrA.* The phosphorylated *AgrA* subsequently collaborates with *SarA* to bind the P2 promoter, which drives expression of the *AgrBDCA* operon and interacts with the neighboring P3 promoter, ultimately regulating biofilm formation[32]. In summary, these finding demonstrates that under high ethanol stress, exogenous QS signaling molecules exert a significant effect on biofilm formation in *L. paracasei* 5. This discovery provides a theoretical foundation for developing QS engineering strategies aimed at enhancing the ethanol stress adaptability of industrial fermentation strains.

3.3. Effect of inhibitors on ethanol tolerance in L. paracasei 5

Having established the role of exogenous AI-2 and AIP in enhancing the ethanol tolerance of LAB, we subsequently evaluated the effects of QS inhibitors on biofilm development and growth kinetics. As shown in Figures 2A-F, the concurrent inhibition of both biomass and biofilm formation upon addition of the AI-2 inhibitor D-galactose indicates that the enhanced ethanol tolerance is specifically mediated through the AI-2. D-Galactose is known to function as a competitive antagonist by binding to the AI-2 receptor site, thereby jamming the communication channel[33]. To investigate the potential role of AIP-mediated QS in biofilm formation by *L. paracasei* 5, we employed pectolinarin, a flavonoid glycoside previously identified as an inhibitor of QS[34]. Notably, while the co-administration of AIP and pectolinarin did not significantly affect the growth of *L. paracasei* 5 (Figures 2G-L), it markedly suppressed biofilm formation. This observation is consistent with earlier reports and can be mechanistically explained by the specific inhibition of the AIP-*AgrC* signaling axis, which selectively disrupts the expression of biofilm-related genes without impairing essential growth functions[34]. Overall, the inhibitor experiments in this study further confirm that AI-2 and AIP signaling molecules can help *L. paracasei* 5 withstand the adverse stress induced by high-ethanol environments, thereby regulating biofilm formation.



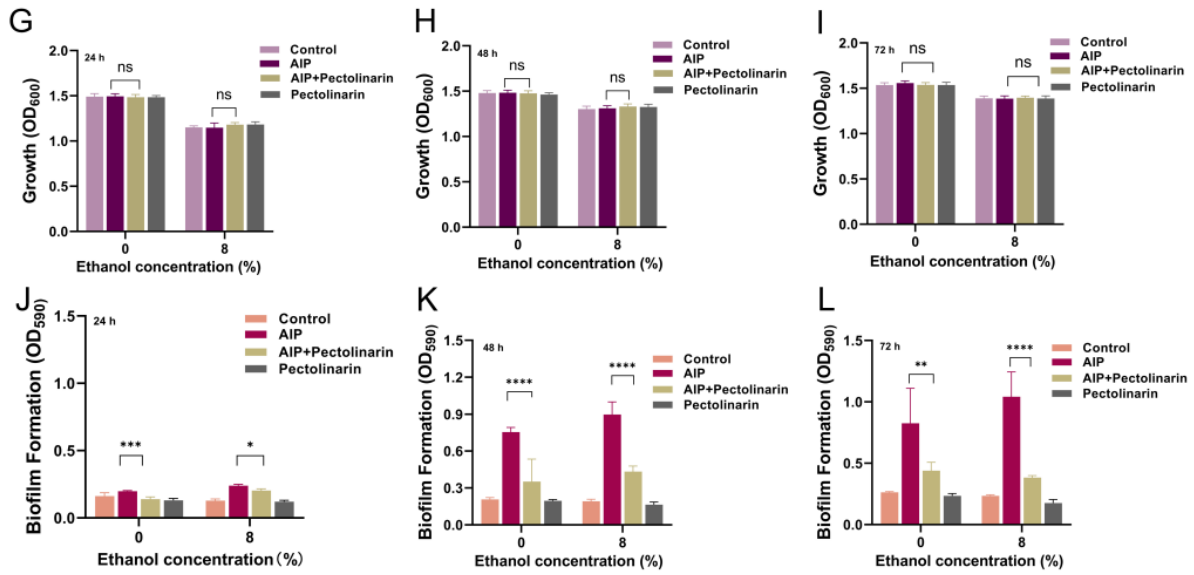


Figure 2. Effects of D-galactose and pectolinarin on *L. paracasei* 5 growth and biofilm throughinhibition of AI-2 and AIP signaling under ethanol stress.(A-C) Growth curves of AI-2-treated *L. paracasei* 5 following additions of D-galactose under 0%and 8% ethanol at 24, 48, and 72 h. (D-F) Biofilm formation in D-galactose treated and controlgroups under the same conditions. (G-I) Growth curves of AIP-treated *L. paracasei* 5 following additions of pectolinarin under 0% and 8% (v/v) ethanol at 24, 48, and 72 h. (J-L) Biofilm formation in pectolinarin treated and control groups under the same conditions. Data were presented as mean± SD (n = 3). Significant differences were determined by two-way ANOVA. *: $P < 0.05$, **: $P < 0.01$, ***: $P < 0.001$, ****: $P < 0.0001$.

3.4. Effect of signaling molecules on the physiological properties of L. paracasei 5 under ethanol environment

In most natural environments, bacterial cells are encapsulated within an EPS matrix, which serves as the primary structural component of biofilms[35]. EPS not only provides a physical framework but also functions as a diffusion barrier, restricting ethanol penetration and conferring mechanical stability to the biofilm structure. Under conditions of elevated ethanol concentrations, the addition of QS signal molecules significantly increased EPS production in *L. paracasei* 5 compared to the control group (Figure 3A). This observation suggests that enhanced EPS synthesis is a critical factor in the development and stabilization of biofilm architecture. These findings indicate that activation of the QS system enables the bacterial population to implement a more effective defense mechanism against ethanol-induced stress by reinforcing the structural integrity and adhesive properties of the biofilm. The results demonstrate that QS activation can enhance biofilm formation under ethanol stress conditions. As membrane homeostasis is essential for cellular integrity and viability, membrane fluidity was assessed next. The incorporation of AI-2 and AIP resulted in a marked decrease in fluorescence anisotropy (γ) in *L. paracasei* 5 (Figure 3B), suggesting a considerable enhancement in membrane fluidity under conditions of ethanol-induced stress. Microstructural observation of *L. paracasei* 5 using SEM revealed striking morphological changes induced by ethanol stress. As depicted in Figure 3C, *L. paracasei* 5 exhibited a short rod shape in the absence of ethanol, but displayed notable elongation when exposed to increasing ethanol concentrations. This phenotype became particularly pronounced at 8% and 10% ethanol concentrations, where the bacteria adopted a distinctive filamentous, rope-like morphology. Most notably, in the presence of exogenous AI-2 or AIP, the bacterial cells no longer appeared as dispersed individuals. Instead, they aggregated into dense, demonstrating significantly enhanced intercellular

adhesion[36]. In summary, the findings indicate that AI-2 and AIP signaling molecules systematically enhance the adaptive capacity of *L. paracasei* 5 under high ethanol stress by promoting EPS synthesis, increasing membrane fluidity, and inducing cellular aggregation.

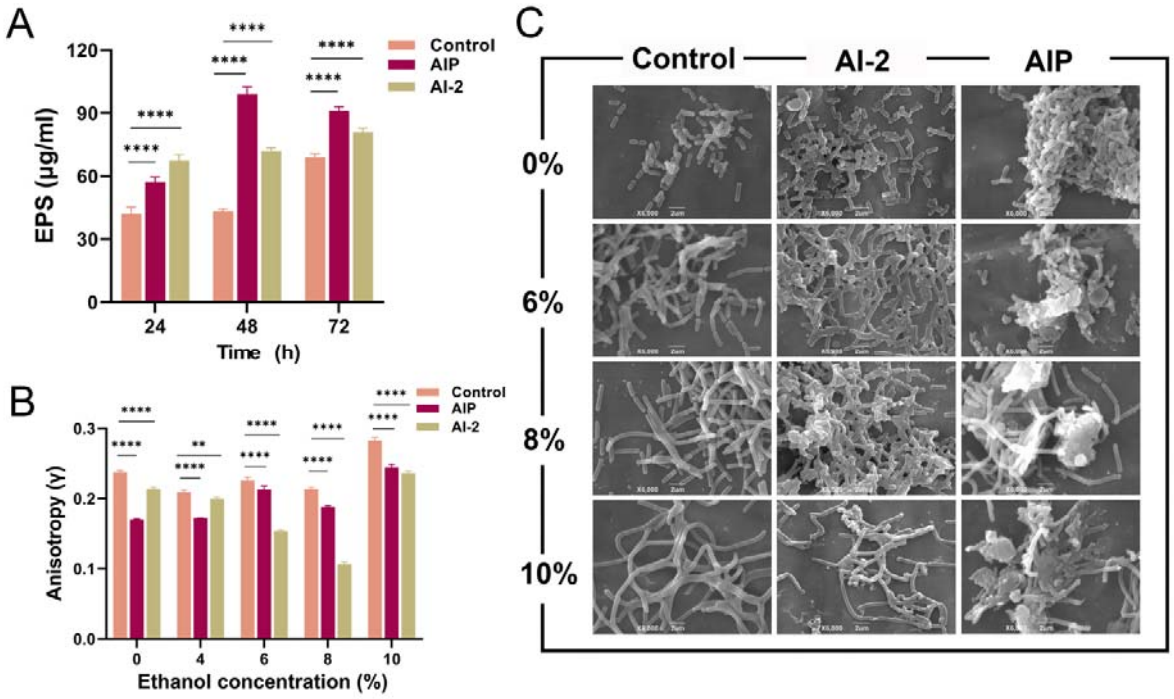


Figure 3. Effects of AI-2 and AIP on EPS production, membrane fluidity, and cell morphology of *L. paracasei* 5.

(A) EPS production by *L. paracasei* 5 in response to exogenous signaling molecules. (B) Membrane fluidity of *L. paracasei* 5 following treatments with exogenous signaling molecules. (C) SEM images showing morphological changes in *L. paracasei* 5 treated with exogenous signaling molecules. Data P <in (A) and (B) were presented as mean ± SD (n = 3). Statistical significance was determined by two-way ANOVA. *: 0.05, **: $P < 0.01$, ***: $P < 0.001$, ****: $P < 0.0001$

3.5. Effect of exogenous signaling molecules on organic acid products of L. paracasei 5

As established, organic acids constitute a key component in the central metabolism of LAB, which are synthesized as part of a complex profile encompassing acetic, lactic, succinic, malic, formic, and citric acids through anaerobic fermentation and other pathways. These compounds extend beyond their role as terminal products of carbon metabolism to act as primary determinants of the bacteria's physiological functionality and application-specific properties[37]. As clearly visualized in Figures 4B and 4D, the AI-2 supplemented group showed markedly higher concentrations of acetic acid and malic acid relative to the untreated control. This metabolic shift can be plausibly attributed to the strains enhanced acetate biosynthesis to maximize ATP yield under high-cell-density conditions, coupled with the concurrent accumulation of malate to maintain intracellular homeostasis[38]. Furthermore, supplementation with the AIP led to significantly elevated levels of malic and citric acids compared to control conditions (Figures 4D and 4E). The accumulation of malate likely contributes to the maintenance of redox balance and cytosolic pH regulation. Additionally, the acidification resulting from organic acid secretion inhibits the growth of competitors such as spoilage and pathogenic microorganisms, thereby facilitating bacterial adhesion to surfaces and promoting the initiation of biofilm formation[39]. In summary, under ethanol stress, the signaling molecules AI-2 and AIP differentially regulate

the organic acid metabolism of *L. paracasei* 5. AI-2 notably enhances the synthesis of acetic and malic acids, which contributes to optimized energy metabolism and intracellular pH homeostasis. In contrast, AIP specifically promotes the accumulation of malic and citric acids, thereby participating in redox balance regulation and inhibiting the growth of competing microorganisms through environmental acidification. Together, these metabolic adaptations enhance the physiological fitness and ecological competitiveness of the strain under high-stress conditions.

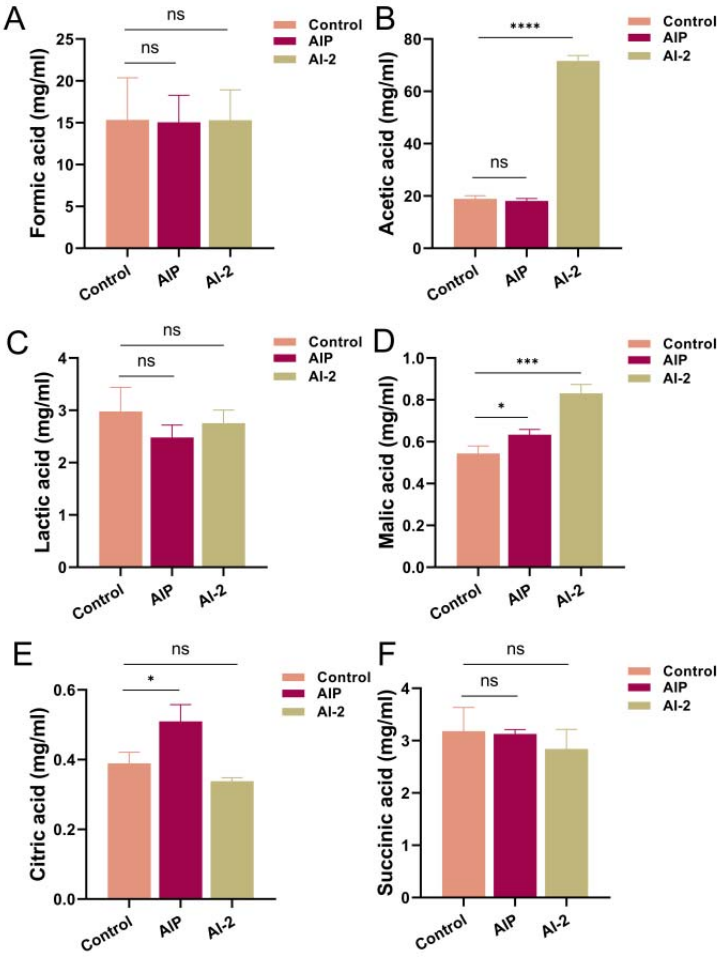


Figure 4. Effects of AIPs and AI-2 on the production of organic acids by L. paracasei 5. (A) Formic acid (B) Acetic acid (C) Lactic acid (D) Malic acid (E) Citric acid (F) Succinic acid. Data was presented as mean ± SD (n = 3). Significant differences were determined by two-way ANOVA. *: $P < 0.05$, **: $P < 0.01$, ***: $P < 0.001$, ****: $P < 0.0001$

3.6. Transcriptome analysis

3.6.1 Transcriptome analysis of AI-2 vs control

To reveal the molecular mechanism by which AIP and AI-2 enhance biofilm formation in *L. paracasei* 5 under ethanol stress, a comparative transcriptomic analysis was performed on strains cultivated in 8% ethanol. A comparative analysis of the transcriptomes revealed a core of 2962 genes commonly expressed in both AI-2-treated and untreated *L. paracasei* 5 (Figure 5A). Additionally, 14 genes were uniquely expressed in the control group, while 10 genes were specifically expressed following AI-2 supplementation. Principal component analysis (PCA) of the transcriptome data revealed a clear segregation between AI-2 and control

samples (Figure 5B). Furthermore, the tight intra-group clustering of biological replicates demonstrated high reproducibility, validating experimental robustness. The subsequent correlation heatmap further illustrated the relationships between samples, revealing coherent clustering within each group. These results confirm the high reliability of the sequencing data (Figure 5C). Differential gene expression analysis was conducted using the DESeq2 algorithm on raw read counts, with significance defined as an adjusted p-value < 0.05 and $|\log_2 FoldChange| > 2$. This approach identified 117 DEGs in response to AI-2 treatment. As depicted in the volcano plot (Figure 5E), the transcriptional landscape was markedly altered, with 72 genes upregulated and 45 downregulated, indicating a comprehensive transcriptomic response to AI-2. Functional classification using the KEGG database demonstrated a significant enrichment of genes in metabolic pathways, particularly in Carbohydrate metabolism, Amino acid metabolism, and Energy metabolism (Figure 5D). This transcriptional profile suggests a metabolic shift geared toward generating ample precursors (e.g., sugars, amino acids) and ATP to energize the biosynthesis of EPS for biofilm formation.

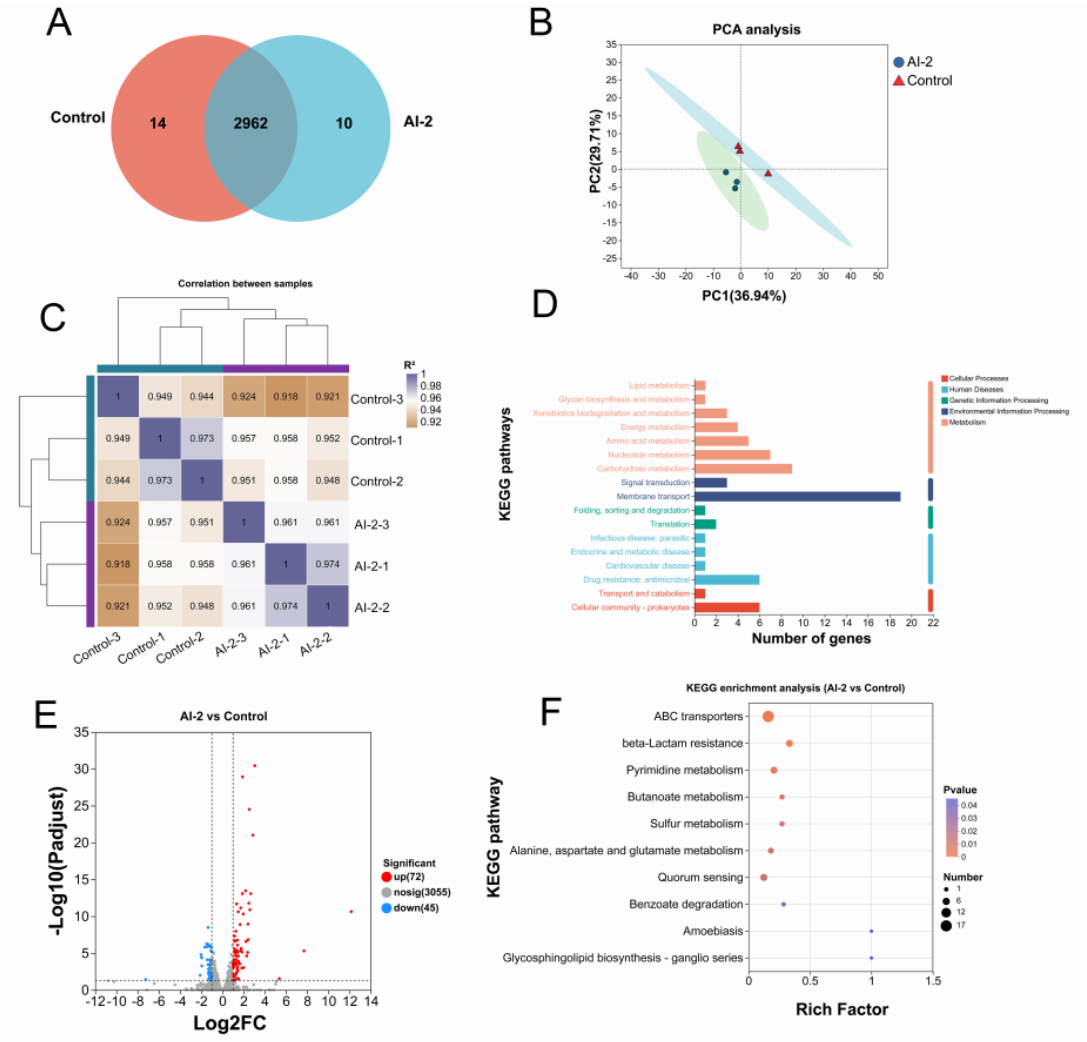


Figure 5. Transcriptome analysis of AI-2 vs control. (A) Venn diagram showing unique and shared DEGs between control and AI-2 treated groups. (B) PCA of transcriptomes demonstrating separation between control and AI-2 groups. (C) Pearson correlation matrix of sample-to-sample relationships. Color intensity reflects correlation coefficients. (D) KEGG pathway annotation of DEGs. (E) Volcano plot of DEGs (red: upregulated; blue: downregulated; gray: non-significant) with significance thresholds ($|\log2FC| > 2$; $P < 0.05$). (F) KEGG enrichment analysis of significantly regulated pathways (top 10 shown).

KEGG pathway enrichment analysis was performed on the DEGs from AI-2 vs control to reveal their functional implications. The top ten significantly enriched pathways are presented in Figure 5F, which included key systems such as signal transduction and energy metabolism. Crucially, the most prominently enriched pathway was ABC transporters. As a primary transmembrane transport system, ABC transporters are indispensable for biofilm development. They enable the export of EPS precursors, which is essential for building the biofilm. This dependency is further amplified under ethanol stress, which disrupts membrane integrity, making ATP-driven transport critical for maintaining cellular homeostasis[40]. Within the ABC transporter system, we observed distinct differential regulation, with the taurine transporter (*TauA/B/C/D*) being downregulated while the spermidine/putrescine (*PotA/B/C/D*), phosphonate (*PhnC/D/E*), and oligopeptide (*OppA/B/C/D/F*) transporters were upregulated (Table 1). This finding is consistent with a previous study[41], which demonstrated that the oligopeptide substrate-binding protein *OppA* enhanced acid stress tolerance in *Limosilactobacillus reuteri*. This parallel suggests a broader role for *Opp* systems in bacterial stress management, indicating that their upregulation in our study likely contributes to the observed ethanol tolerance in *L. paracasei* 5.

Table 1 KEGG enrichment analysis of genes differentially expressed by AI-2 in *L. paracasei* 5.

Pathway ID	Pathway Description	Gene
map02010	ABC transporters	*TauA*、*TauC*、*TauB*、*PotD*、*PotC*、*PotB*、*PotA*、*PhnD*、*PhnE*、*PhnC*、*OppA*、*OppB*、*OppC*、*OppD*、*OppF*
map01501	beta-Lactam resistance	*OppA*、*OppB*、*OppC*、*OppD*、*OppF*
map00240	Pyrmidine metabolism	*pyrB*、*pyrC*、*pyrG*、*carA*、*rtpR*、*pyrR*
map00650	Butanoate metabolism	*adhE*、*madB*、*gcdC*
map00920	Sulfur metablism	*TauA*、*TauC*、*TauB*
map00250	Alanine,aspartate and glutamate metabolism	*pyrB*、*purA*、*carA*
map02024	Quorum sensing	*OppA*、*OppB*、*OppC*、*OppD*、*OppF*
map00626	Naphthalene degradation	*adhE*
map00071	Fatty acid degradation	*adhE*
map00625	Chloroalkane and chloroalkene degradation	*adhP*
map04931	Insulin resistance	*glmS*
map00051	Fructose and mannose metabolism	*cmtB*
map00350	Tyrosine metabolism	*adhE*
map00620	Pyruvate metabolism	*madB*、*adhE*
map00910	Nitrogen metabolism	*caH*
map02020	Two-component system	*CitC*、*CitD*、*CitE*
map00230	Purine metabolism	*rtpR*、*purA*
map00520	Amino sugar and nucleotide sugar metabolism	*nagZ*、*glmS*
map00970	Aminoacyl-tRNA biosynthesis	*hisS*
map00010	Glycolysis / Gluconeogenesis	*adhE*
map02060	Phosphotransferase system (PTS)	*cmtB*、*fruK*
map03010	Ribosome	*rpmF*

Besides, the QS pathway was significantly enriched, providing direct evidence for AI-2-mediated genetic regulation. This finding indicates that bacterial cells sense population density and initiate coordinated group behaviors, including biofilm formation. The QS system directly regulates biofilm-related genes, such as *Opp*, *Opp/Ami*, *PrgZ/Opp*, *TraC/Opp*. QS modulates gene expression in response to cell density through autoinducer molecules such as acyl-homoserine lactones (AHLs) and AI-2, thereby activating genes associated with EPS production, adhesion, virulence, and stress resistance[42]. Furthermore, QS facilitates

population-level synchronization, enhances cell-to-cell adhesion, and stabilizes the biofilm matrix[43]. In addition, core metabolic pathways, including pyrimidine, butyrate, sulfur, alanine, aspartate, and glutamate metabolism, were significantly enriched. Sulfur metabolism, which is required for the incorporation of sulfur into the amino acids cysteine and methionine, was also enriched. Critically, these amino acids serve as key precursors for the synthesis of the AI-2 signal molecule itself, as demonstrated previously[44]. Consequently, the enhanced sulfur metabolism induced by AI-2 not only supports the QS but may also alleviate a critical metabolic bottleneck and thus contribute to the observed improvement in ethanol tolerance.In summary, transcriptomic analysis clarified the molecular basis underlying the physiological adaptations observed in *L. paracasei* 5 under ethanol stress. The differential expression of the ABC transporter family serves as a core regulatory node mediating stress tolerance, EPS synthesis, and biofilm formation in this strain. The significant upregulation of *PotA/B/C/D*, *PhnC/D/E*, and *OppA/B/C/D/F*, coupled with the downregulation of *TauA/B/C/D*, collectively constructs a metabolic pathway centered on ATP-driven transport. This pathway provides crucial material and energy support for the synthesis of biofilm matrix components under the regulation of AI-2.

3.6.2 Transcriptome analysis of AIP vs control

To investigate the regulatory function of the AIP-mediated QS system in *L. paracasei* 5, we conducted transcriptomic profiling of cells treated with AIP. As illustrated in the Venn diagram (Figure 6A), 2957 genes were co-expressed in both the AIP-treated and control groups, while 19 genes were uniquely expressed in the control group and 5 genes were specific to the AIP group. PCA revealed clear segregation between the AIP and control samples (Figure 6B), indicating a distinct transcriptomic response induced by AIP. Furthermore, inter-sample correlation heatmap analysis demonstrated strong reproducibility among biological replicates within each group, reaffirming the high reliability of the sequencing data (Figure 6C). Based on these results, differential expression analysis identified 88 DEGs in the AIP-treated group, comprising 51 upregulated and 37 downregulated genes (Figure 6E). Subsequently, KEGG pathway enrichment analysis was performed to elucidate the potential functions and key pathways involving these DEGs. Figure 6D showed significant enrichment of these genes in 11 specific pathways, grouped into five functional categories: Metabolism, Environmental Information Processing, Genetic Information Processing, Human Diseases, and Cellular Processes. KEGG pathway enrichment analysis of the DEGs between AIP and control groups was performed to elucidate the functional basis of AIP-induced phenotypes. The top ten significantly enriched pathways are presented in Figure 6F, with ABC transporters and the PTS being the most prominent. Within the ABC transporter pathway, key genes encoding substrate-binding and permease components (including *OppC, PotC, PotB*, and *PotD*) were significantly upregulated. This coordinated enhancement suggests a functional amplification of the ABC transporter system, empowering the bacteria to actively import critical nutrients and export harmful substances. This ATP-driven process is essential for maintaining cellular homeostasis under high ethanol stress, ultimately contributing to the improved survival rate of *L. paracasei* 5 in high-ethanol environments.

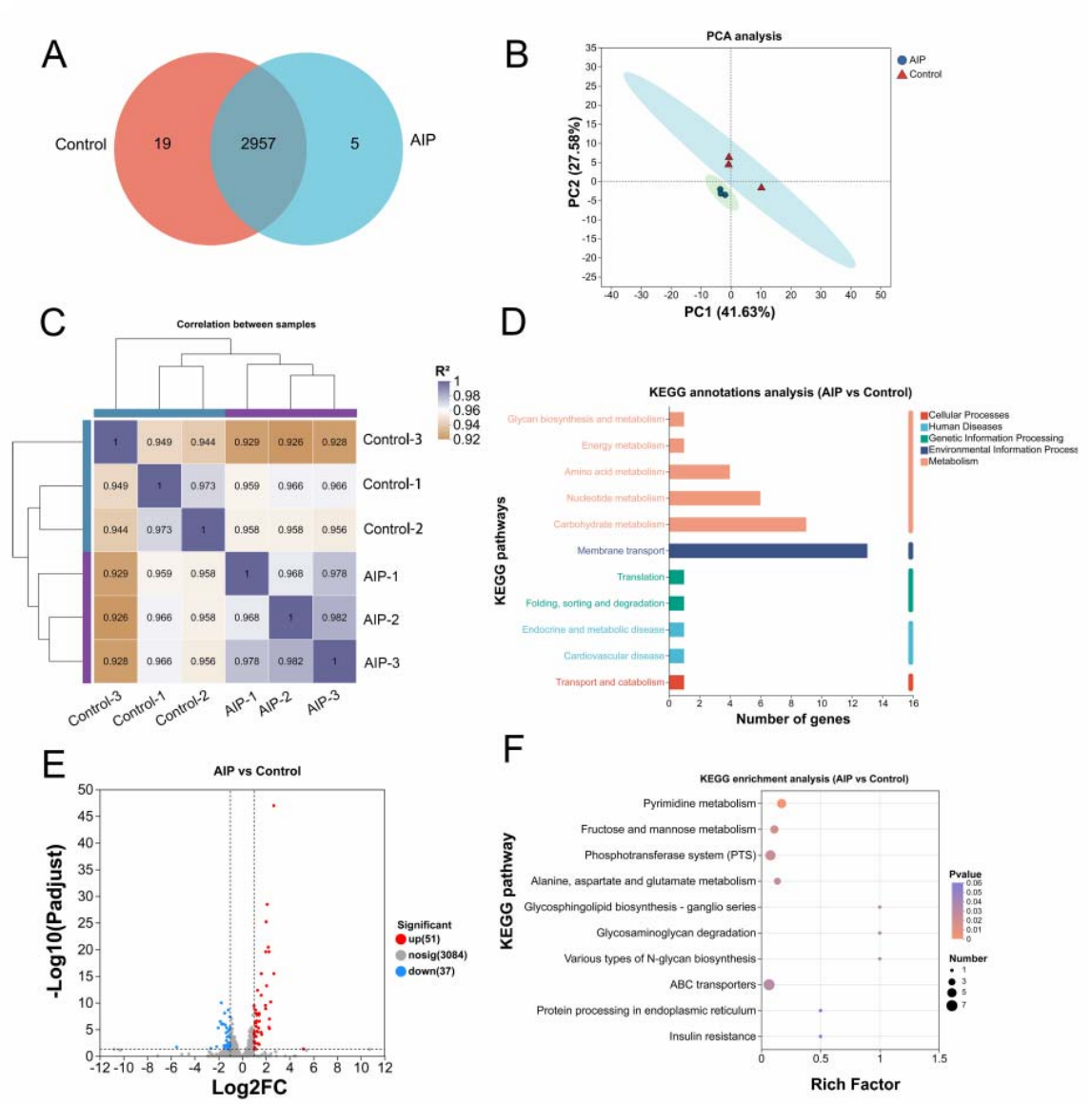


Figure 6. Transcriptome analysis of AIP vs control. (A) Venn diagram showing unique and shared DEGs between control and AIP treated groups. (B) PCA of transcriptomes demonstrating separation between control and AIP groups. (C) Pearson correlation matrix of sample-to-sample relationships. Color intensity reflects correlation coefficients. (D) KEGG pathway annotation of DEGs. (E) Volcano plot of DEGs (red: upregulated; blue: downregulated; gray: non-significant) with significance thresholds (|log2FC| > 2; 0.05). (F) KEGG enrichment analysis of significantly regulated pathways (top 10 shown).

KEGG enrichment analysis revealed the significant upregulation of the PTS, a primary carbohydrate transport system in Gram-positive bacteria. Specific PTS component genes (e.g., *BglF*, *MtlA*, *CelB*, *CelC*) were markedly upregulated (Table 2). The PTS facilitates the concurrent transport and phosphorylation of sugars such as glucose and mannose, thereby efficiently generating phosphorylated intracellular substrates for glycolysis and EPS biosynthesis[45]. Concurrently, pathways for carbohydrate metabolism, particularly fructose and mannose metabolism, were significantly enriched. The upregulation of these pathways is critical for generating ATP, NADH, and various biosynthetic precursors[46]. The transcriptional upregulation of these EPS-related pathways provides direct evidence that AIP supplementation enhances the biosynthesis of biofilm-associated components in *L. paracasei* SB725[43]. This elevated metabolic activity is critical for the structural integrity, stress resilience, and long-term maintenance of the biofilm, underscoring the role of

AIP-mediated QS in promoting bacterial survival under adverse environmental conditions. In summary, transcriptomic profiling of AIP-treated *L. paracasei* 5 revealed that AIP-mediated QS orchestrates a coordinated transcriptional response centered on enhancing nutrient acquisition and metabolic adaptation. The significant upregulation of ABC transporters (e.g., *OppC*, *PotB-D*) and the PTS (e.g., *BglF*, *MtlA*) underpins the improved uptake of carbohydrates and oligopeptides, which serve as critical substrates for energy metabolism and EPS biosynthesis[47]. These molecular adjustments are further supported by the enrichment of carbohydrate metabolism pathways, collectively driving the synthesis of biofilm matrix components and providing the metabolic foundation for enhanced biofilm structural integrity and ethanol stress resilience. This transcriptional reprogramming elucidates how AIP signaling reconfigures cellular physiology to promote survival in high-ethanol environments, reinforcing the role of QS as a key regulator of functional adaptation in LAB.

Table 2 KEGG enrichment analysis of genes differentially expressed by AIP in *L. paracasei* 5.

Pathway ID	Pathway Description	Gene
map00240	Pyrimidine metabolism	*pyrC*、*pyrB*、*pyrG*、*pyrR*、*nrdA*
map02010	ABC transporters	*PotD*、*PotC*、*PotB*、*PotA*、*ugpE*、*PhnD*、*PhnC*
map00513	Various types of N-glycan biosynthesis	*HEXO1*
map00250	Alanine, aspartate and glutamate metabolism	*pyrB*、*purA*、*glmS*
map04141	Protein processing in endoplasmic reticulum	*sHSF*
map04931	Insulin resistance	*glmS*
map02060	Phosphotransferase system (PTS)	*cmtB*、*celB*、*celC*、*fruA*、*fruB*、*fruK*
map00051	Fructose and mannose metabolism	*cmtB*、*fruA*、*mtlD*、*fruK*
map00603	Glycosphingolipid biosynthesis - globo and isoglobo series	*HEXO1*
map04142	Lysosome	*HEXO1*
map00910	Nitrogen metabolism	*cah*
map00630	Glyoxylate and dicarboxylate metabolism	*eda*
map00500	Starch and sucrose metabolism	*celB*、*celC*
map00300	Lysine biosynthesis	*dapE*
map00520	Amino sugar and nucleotide sugar metabolism	*glmS*、*nagZ*
map00230	Purine metabolism	*nrdA*
map00030	Pentose phosphate pathway	*eda*
map03010	Ribosome	*rpsU*

This study offers mechanistic insights through transcriptomic analysis; however, several limitations must be acknowledged. Firstly, while our findings indicate a significant association between exogenous QS signaling molecules (AI-2 and AIP) and enhanced biofilm formation under ethanol stress, the data are predominantly correlational. To establish direct causal relationships between QS pathways and the observed phenotypes, further experimental validation is necessary, such as through gene knockdown or overexpression studies. Secondly, this research was conducted under controlled in vitro conditions. Although this approach ensures experimental reproducibility, the findings may not be directly applicable to complex and dynamically changing environments, such as actual food fermentation systems or the gastrointestinal tract, where multiple stress factors (e.g., low pH, oxidative stress, nutrient limitation, and competitive microbial communities) coexist and interact. Ultimately, transcriptomic analysis was conducted at a singular time point. While this method effectively captures the cellular state at a specific moment, it fails to offer a dynamic perspective on

biofilm formation and stress adaptation. Future research addressing these limitations will enhance our comprehension of QS-mediated stress tolerance in LAB.

4. Conclusion

In summary, this study demonstrates that exogenous QS signals, AI-2 and AIP, enhance ethanol tolerance in *L. paracasei* 5 through distinct molecular pathways. *L. paracasei* 5 treated with AI-2 or AIP exhibited enhanced biofilm formation, increased membrane fluidity, and stimulated EPS production, which constitute functional adaptations critical for maintaining cellular integrity under ethanol stress. Transcriptomic profiling revealed that AI-2 primarily functions through upregulation of ABC transporter genes, including *PotABCD*, *PhnCDE*, and *OppABCDF*, optimizing the uptake of polyamines, phosphonates, and oligopeptides critical for stress resilience and biofilm matrix assembly. Conversely, AIP primarily activates components of the PTS, including *BglF*, *MtlA*, *CelB*, and *CelC*, thereby enhancing carbohydrate uptake and fueling central carbon metabolism to meet the biosynthetic demands of biofilm development (Figure 7). These findings systematically elucidate the mechanistic basis of QS-mediated stress adaptation in bacteria and provide a theoretical foundation for developing novel strategies to enhance industrial strain robustness through QS modulation.

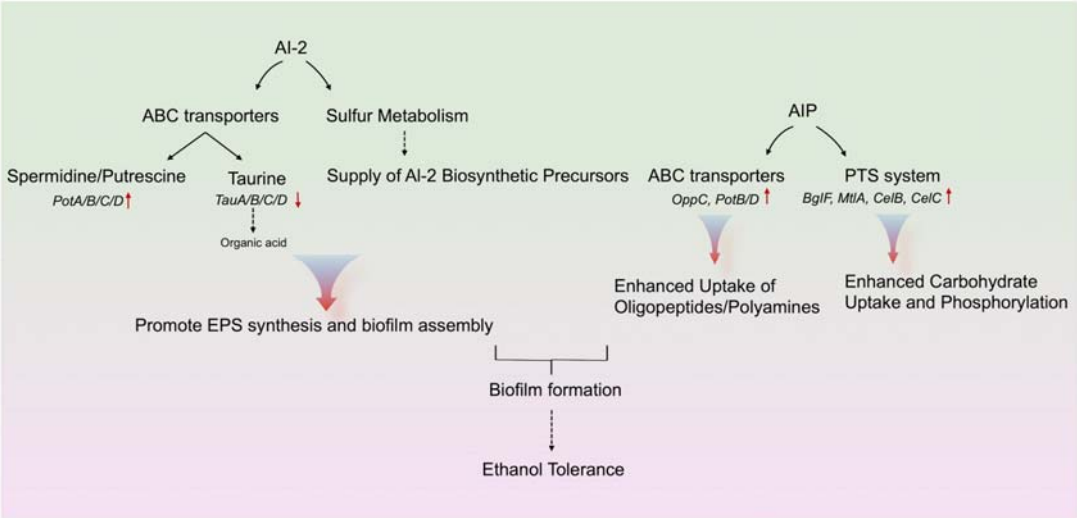


Figure 7. Potential mechanisms of ethanol tolerance mediated by AI-2 and AIP in *L. paracasei* 5

Declaration of competing interest

The authors state that there are no known competing financial interests or personal relationships that could have appeared to influence the work reported in this paper.

Acknowledgements

We acknowledge financial support from the National Key Research and Development Program of China (2024YFF1106100), the National Natural Science Foundation of China (No. 32272299), and Open Project Funding of the Key Laboratory of Fermentation Engineering (Ministry of Education) (202409FE07).

References

[1] VAN WYK J. Kefir: The Champagne of Fermented Beverages [M]. Fermented Beverages. 2019: 473-527.

[2] WANG Y, XIE Z, DU L, et al. Heat-killed *Lacticaseibacillus paracasei* 6235 is more effective than live on DSS-induced colitis via modulation of intestinal microbiota and MAPK/NF-κB signaling pathways [J]. Food & Function, 2025.

[3] LEVANTE A, FOLLI C, MONTANINI B, et al. Expression of DinJ-YafQ System of *Lactobacillus casei* Group Strains in Response to Food Processing Stresses [J]. Microorganisms, 2019.

[4] REALE A, DI RENZO T, ROSSI F, et al. Tolerance of Lactobacillus casei, L*actobacillus paracasei* and *Lactobacillus rhamnosus* strains to stress factors encountered in food processing and in the gastro-intestinal tract [J]. LWT - Food Science and Technology, 2015.

[5] BUSTOS A Y, TARANTO M P, GEREZ C L, et al. Recent Advances in the Understanding of Stress Resistance Mechanisms in Probiotics: Relevance for the Design of Functional Food Systems [J]. Probiotics and Antimicrobial Proteins, 2024.

[6] RIVAS G A, FLORES N E, BRIZUELA N S, et al. Novel Malolactic Fermentation Starter Formulated Using Native Lactic Acid Bacteria Strains from a Re-Emerging Wine-Growing Region of Argentina—A Pilot Scale Vinification [J]. Fermentation, 2025, 11(3).

[7] DA CRUZ NIZER W S, ALLISON K N, ADAMS M E, et al. The role of exopolysaccharides Psl and Pel in resistance of Pseudomonas aeruginosa to the oxidative stressors sodium hypochlorite and hydrogen peroxide [J]. Microbiology Spectrum, 2024.

[8] KUBOTA H, SENDA S, NOMURA N, et al. Biofilm formation by lactic acid bacteria and resistance to environmental stress [J]. Journal of Bioscience and Bioengineering, 2008.

[9] MONDAL S, MELZI A, ZECCHIN S, et al. Quorum sensing in biofilm-mediated heavy metal resistance and transformation: environmental perspectives and bioremediation [J]. Frontiers in Microbiology, 2025.

[10] SHOJIMA A, NAKAYAMA J. Quorum sensing in gram-positive bacteria: assay protocols for staphylococcal agr and enterococcal fsr systems [J]. Methods in Molecular Biology, 2014.

[11] BORGES A, SOUSA P, GASPAR A, et al. Furvina inhibits the 3-oxo-C12-HSL-based quorum sensing system of Pseudomonas aeruginosa and QS-dependent phenotypes [J]. Biofouling, 2017.

[12] WANG Y, LIU B, GRENIER D, et al. Regulatory Mechanisms of the LuxS/AI-2 System and Bacterial Resistance [J]. Antimicrobial Agents and Chemotherapy, 2019.

[13] GAO M, SONG H, ZHENG H, et al. Culture of low density E. coli cells in alginate-chitosan microcapsules facilitates stress resistance by up-regulating luxS/AI-2 system [J]. Carbohydrate Polymers, 2016.

[14] CHEN Y, FAN X, ZHU X, et al. Effects of luxS gene on biofilm formation and fermentation property in *Lactobacillus plantarum* R [J]. Food Research International, 2025.

[15] GU Y, TIAN J, ZHANG Y, et al. Dissecting signal molecule AI-2 mediated biofilm formation and environmental tolerance in *Lactobacillus plantarum* [J]. Journal of Bioscience and Bioengineering, 2020.

[16] LI H, LI X, WANG Z, et al. Autoinducer-2 regulates Pseudomonas aeruginosa PAO1 biofilm formation and virulence production in a dose-dependent manner [J]. BMC Microbiology, 2015.

[17] TU Y, LI H, HUO J, et al. Disrupting the bacterial language: quorum quenching and its applications [J]. Critical Reviews in Microbiology, 2025.

[18] WATERS C M, BASSLER B L. Quorum sensing: cell-to-cell communication in bacteria [J]. Annual Review of Cell and Developmental Biology, 2005.

[19] HAN X G, LU C P. In vitro biosynthesis of autoinducer 2 of Steptococcus suis Serotype 2 using recombinant LuxS and Pfs [J]. Enzyme and Microbial Technology, 2009, 44(1): 40-5.

[20] GU Y, WU J, TIAN J, et al. Effects of Exogenous Synthetic Autoinducer-2 on Physiological Behaviors and Proteome of Lactic Acid Bacteria [J]. ACS Omega, 2020.

[21] PéREZ-CHABELA M L, DíAZ-VELA J, REYES-MENéNDEZ C V, et al. Improvement of Moisture Stability and Textural Properties of Fat and Salt Reduced Cooked Sausages by Inoculation of Thermotolerant Lactic Acid Bacteria [J]. International Journal of Food Properties, 2013, 16(8): 1789-808.

[22] FREEMAN C D, HANSEN T, URBAUER R, et al. Defective pgsA contributes to increased membrane fluidity and cell wall thickening in Staphylococcus aureus with high-level daptomycin resistance [J]. mSphere, 2024.

[23] TIWARI K B, SEN S, GATTO C, et al. Fluorescence Polarization (FP) Assay for Measuring Staphylococcus aureus

Membrane Fluidity [J]. Methods in molecular biology (Clifton, NJ), 2021.

[24] YADAV M K, SONG J H, VASQUEZ R, et al. Methods for Detection, Extraction, Purification, and Characterization of Exopolysaccharides of Lactic Acid Bacteria-A Systematic Review [J]. Foods, 2024, 13(22).

[25] HENKE J M, BASSLER B L. Three parallel quorum-sensing systems regulate gene expression in Vibrio harveyi [J]. Journal of Bacteriology, 2004.

[26] HENKE J M, BASSLER B L. Quorum sensing regulates type III secretion in Vibrio harveyi and Vibrio parahaemolyticus [J]. Journal of Bacteriology, 2004.

[27] LIN S, WANG L, LIU J, et al. Second-generation bioenergy to decouple fossil fuel dependency and environmental deterioration: Dynamic and optimal mechanisms and gas-to-ash products of combustion of Pennisetum hydridum [J]. Biomass & Bioenergy, 2024.

[28] CAO H, WEI D, YANG Y, et al. Systems-level understanding of ethanol-induced stresses and adaptation in E. coli [J]. Scientific Reports, 2017.

[29] INGRAM L O. Ethanol tolerance in bacteria [J]. Critical Reviews in Biotechnology, 1990.

[30] HE S, ZHAN Z, SHI C, et al. Ethanol at Subinhibitory Concentrations Enhances Biofilm Formation in Salmonella enteritidis [J]. Foods, 2022.

[31] LI M, LI B, LONG B, et al. Harnessing exogenous AI-2 to improve ethanol tolerance in *Lactobacillus plantarum* R: Insights from transcriptome and metabolome [J]. Lwt, 2025, 231.

[32] WANG Y, BIAN Z, WANG Y. Biofilm formation and inhibition mediated by bacterial quorum sensing [J]. Appl Microbiol Biotechnol, 2022, 106(19-20): 6365-81.

[33] RYU E-J, SIM J, SIM J, et al. D-Galactose as an autoinducer 2 inhibitor to control the biofilm formation of periodontopathogens [J]. Journal of Microbiology, 2016.

[34] KIM D, KIM K-Y. Pectolinarin Inhibits the Bacterial Biofilm Formation and Thereby Reduces Bacterial Pathogenicity [J]. Antibiotics, 2022.

[35] GU Y, TIAN J, ZHANG Y, et al. Dissecting signal molecule AI-2 mediated biofilm formation and environmental tolerance in *Lactobacillus plantarum* [J]. Journal of Bioscience and Bioengineering, 2021, 131(2): 153-60.

[36] VAN BOKHORST-VAN DE VEEN H, ABEE T, TEMPELAARS M, et al. Short- and long-term adaptation to ethanol stress and its cross-protective consequences in *Lactobacillus plantarum* [J]. Applied and Environmental Microbiology, 2011.

[37] WANG Y, XIA K, WANG X N, et al. Improvement of feed intake, digestibility, plasma metabolites, and lactation performance of dairy cows fed mixed silage of sugar beet pulp and rice straw inoculated with lactic acid bacteria [J]. Journal of Dairy Science, 2021.

[38] LIU X, FU J, MA W, et al. Screening and evaluation of high stress tolerance, high esterase activity and safety of Oenococcus oeni strains adapt to challenging conditions in Northwest China wine [J]. LWT - Food Science and Technology, 2024.

[39] AKBAS M Y, CAG S. Use of organic acids for prevention and removal of Bacillus subtilis biofilms on food contact surfaces [J]. Food Sci Technol Int, 2016, 22(7): 587-97.

[40] FOO J L, JENSEN H M, DAHL R H, et al. Improving microbial biogasoline production in Escherichia coli using tolerance engineering [J]. mBio, 2014.

[41] WANG G, LI D, MA X, et al. Functional role of oppA encoding an oligopeptide-binding protein from *Lactobacillus salivarius* Ren in bile tolerance [J]. Journal of Industrial Microbiology & Biotechnology, 2015.

[42] JINGJING E, RONGZE M, ZICHAO C, et al. Improving the freeze-drying survival rate of *Lactobacillus plantarum* LIP-1 by increasing biofilm formation based on adjusting the composition of buffer salts in medium [J]. Food Chem, 2021, 338: 128134.

[43] LIU Y, LIU Y, CAO J, et al. Comparative transcriptomic analysis of biofilm formation mechanism in *Lacticaseibacillus paracasei* SB27 [J]. Food Bioscience, 2025, 72.

[44] JU X, LI J, ZHU M, et al. Effect of the luxS gene on biofilm formation and antibiotic resistance by Salmonella serovar Dublin [J]. Food Research International, 2018.

[45] LI L, ZHANG H, MENG D, et al. Transcriptomics of *Lactobacillus paracasei*: metabolism patterns and cellular responses under high-density culture conditions [J]. Frontiers in Bioengineering and Biotechnology, 2023.

[46] MILANOVIC V, CIANI M, ORO L, et al. Starmerella bombicola influences the metabolism of Saccharomyces cerevisiae at pyruvate decarboxylase and alcohol dehydrogenase level during mixed wine fermentation [J]. Microbial Cell Factories, 2012.

[47] GAO T, DING M, YANG C-H, et al. The phosphotransferase system gene ptsH plays an important role in MnSOD production, biofilm formation, swarming motility, and root colonization in Bacillus cereus 905 [J]. Research in Microbiology, 2018.